tMolecular Biology of the Cell
Vol. 11, 241–253, January 2000

Functional Coordination of Three Mitotic Motors in *Drosophila* Embryos[V]

David J. Sharp, Heather M. Brown, Mijung Kwon, Gregory C. Rogers, Gina Holland, and Jonathan M. Scholey*

Section of Molecular and Cellular Biology, University of California-Davis, Davis, California 95616

Submitted September 9, 1999; Revised October 25, 1999; Accepted October 28, 1999
Monitoring Editor: J. Richard McIntosh

It is well established that multiple microtubule-based motors contribute to the formation and function of the mitotic spindle, but how the activities of these motors interrelate remains unclear. Here we visualize spindle formation in living *Drosophila* embryos to show that spindle pole movements are directed by a temporally coordinated balance of forces generated by three mitotic motors, cytoplasmic dynein, KLP61F, and Ncd. Specifically, our findings suggest that dynein acts to move the poles apart throughout mitosis and that this activity is augmented by KLP61F after the fenestration of the nuclear envelope, a process analogous to nuclear envelope breakdown, which occurs at the onset of prometaphase. Conversely, we find that Ncd generates forces that pull the poles together between interphase and metaphase, antagonizing the activity of both dynein and KLP61F and serving as a brake for spindle assembly. During anaphase, however, Ncd appears to have no effect on spindle pole movements, suggesting that its activity is down-regulated at this time, allowing dynein and KLP61F to drive spindle elongation during anaphase B.

INTRODUCTION

The segregation of chromosomes during mitosis depends on the action of a self-organizing, bipolar machine called the mitotic spindle. It is now established that the formation and function of the mitotic spindle requires numerous microtubule (MT)-based motor proteins (Hoyt and Geiser, 1996; Vale and Fletterick, 1997). Although the identities of many of these mitotic motors are becoming clear, their specific functional interrelationships have been extremely difficult to ascertain.

Among all mitotic movements, the positioning of spindle poles during the assembly and elongation of the bipolar mitotic spindle may require the greatest degree of cooperation between different motors. This process is particularly complex because it occurs in a pathway consisting of several, temporally distinct stages, during which the organization of spindle microtubules and the general environment of the cell change dramatically (McIntosh and McDonald, 1989). The members of at least three families of MT motors are thought to play important roles in this pathway. These are the bipolar kinesins, the C-terminal kinesins, and cytoplasmic dynein.

The bipolar (or BimC) kinesins (Vale and Fletterick, 1997) comprise a family of plus-end–directed motors, which have a bipolar morphology with motor domains at both ends of a central rod (Cole *et al.*, 1994; Kashina *et al.*, 1996a,b; Gordon and Roof, 2000). Functionally, these motors are thought to play a role in either the assembly or maintenance of spindle bipolarity, because their inhibition results in the formation of monopolar mitotic spindles (Enos and Morris, 1990; Hagan and Yanagida, 1990; Roof *et al.*, 1991; Hoyt *et al.*, 1992; Sawin *et al.*, 1992; Heck *et al.*, 1993; Blangy *et al.*, 1995; Sharp *et al.*, 1999b). Support for a role for bipolar kinesins in spindle maintenance but not assembly comes from the recent findings that inhibiting the *Drosophila* bipolar kinesin KLP61F does not prevent the initial separation of spindle poles but results in their collapse after nuclear envelope breakdown (NEB) (Sharp *et al.*, 1999b). Immunoelectron microscopy analyses have also shown that KLP61F motors cross-link spindle MTs within interpolar MT bundles (Sharp *et al.*, 1999a), consistent with the hypothesis that these motors exert their effects by sliding antiparallel MTs in relation to one another to push the poles apart. Bipolar kinesins have also been shown to play a role during anaphase B spindle elongation in budding yeast, perhaps by invoking a similar "sliding filament mechanism" (Saunders *et al.*, 1995; Straight *et al.*, 1998).

The C-terminal kinesins comprise a family of minus-end–directed mitotic motors, which have been proposed to exert forces that antagonize bipolar kinesin activity during mitosis (Endow *et al.*, 1990, 1994; Walker *et al.*, 1990; McDonald and Goldstein, 1990; McDonald *et al.*, 1990; Meluh and Rose, 1990; Saunders and Hoyt, 1992; Saunders *et al.*, 1997; Hoyt *et al.*, 1993; O'Connell *et al.*, 1993; Pidoux *et al.*, 1996; Sharp *et al.*, 1999b). Although the mechanism of action of C-terminal

[V] Online version contains video material for Figures 1, 4, and 7. Online version available at www.molbiolcell.org.

* Corresponding author. E-mail address: jmscholey@ucdavis.edu.

kinesins remains controversial, several members of this family, including Ncd from *Drosophila*, are known to cross-link MTs in vitro (McDonald *et al.*, 1990; Chandra *et al.*, 1993; Pidoux *et al.*, 1996; Narasimhulu and Reddy, 1998; Karabay and Walker, 1999). Interestingly, like KLP61F, Ncd also localizes to interpolar microtubule bundles within embryonic spindles (Endow and Komma, 1996). Thus it has been proposed that both Ncd and KLP61F cross-link and slide antiparallel spindle MTs, generating counterbalancing forces, with KLP61F pushing the poles apart and Ncd pulling them together (Sharp *et al.*, 1999b).

Cytoplasmic dynein is a large, multimeric, minus-end–directed motor that is involved in numerous cellular events including mitosis (Karki and Holzbaur, 1999). Several lines of evidence suggest that dynein positions spindle poles during spindle assembly and elongation. These include the observations that the microinjection of antibodies inhibiting dynein function into mammalian cells gives rise to monoastral spindles containing side-by-side spindle poles (Vaisberg *et al.*, 1993) and that dynein null mutants in budding yeast display defects in spindle elongation during anaphase B (Saunders *et al.*, 1995). A very recent study has also shown that hypomorphic mutations of the dynein heavy chain in *Drosophila* inhibits spindle pole separation in early embryos (Robinson *et al.*, 1999). Although it is plausible that dynein motors function during mitosis by driving MT–MT sliding as they do in the ciliary axoneme (Heald *et al.*, 1996), there is also evidence that dynein becomes anchored on the cell cortex (Bloom *et al.*, 1999) where it could slide astral MTs relative to the fixed cortex to separate the poles (Karsenti *et al.*, 1996).

In this study, we use time-lapse confocal microscopy of living, fluorescent tubulin-labeled *Drosophila* embryos in the presence and absence of specific inhibitors of the bipolar kinesin KLP61F, the C-terminal kinesin Ncd, and cytoplasmic dynein. This has allowed us to assess, quantitatively, how the activities of these motors are coordinated to position spindle poles during the pathway of spindle assembly, maintenance, and elongation. Our findings indicate that KLP61F and dynein act on distinct subsets of spindle MTs to generate complementary forces that push and pull the poles apart, respectively. Ncd, on the other hand, antagonizes both motors by acting as a brake for spindle pole separation at all stages through metaphase.

MATERIALS AND METHODS

Drosophila Stocks and Embryo Collections

Flies were maintained and embryos were collected in our laboratory facility as previously described (Sharp *et al.*, 1999a,b). Ca^{nd} (Ncd null allele resulting from a radiation-induced deletion within the gene encoding the motor; Lewis and Gencarella, 1952) flies were provided by R. Scott Hawley. To generate Ncd null embryos, homozygous ca^{nd} females were mated with homozygous ca^{nd} males.

Antibody Preparation

The preparation of the anti-KLP61F and anti-tubulin antibodies was described previously (Sharp *et al.*, 1999a,b). The mAb against the dynein heavy chain was generated by injecting mice with bulk preparations of *Drosophila* MT-associated proteins (MAPs). Individual clones were isolated and grown by standard methods (Harlow and Lane, 1988). The specificity of clones against the dynein heavy chain was determined by Western blots on crude *Drosophila* cytosol, purified MAP preparations, and fractions of these preparations containing only the purified dynein holoenzyme (Hays *et al.*, 1994). Before injection, the antibody was purified from mouse ascites fluid on a protein A column (Bio-Rad, Hercules, CA) and then concentrated to between 8 and 22 mg/ml by spin filtration using Nanosep spin concentration columns with a 10-kDa cutoff (Pall Filtron, Northborough, MA).

Bacterial Expression and Purification of Human p50 Dynamitin

Human p50 dynamitin was cut from a pET14b expression plasmid using *Nco*I and *Eco*RI restriction enzymes, subcloned directionally into a pRSETB (His)6/T7 tag expression plasmid (Invitrogen, Carlsbad, CA), and transformed into a BL21(DE3) bacterial expression strain. Recombinant p50 was expressed and purified in injection buffer (150 mM potassium aspartate, 10 mM potassium phosphate, 20 mM imidazole, pH 7.2) under nondenaturing conditions on Ni-nitrilotriacetic acid Superflow resin (Qiagen, Valencia, CA) using standard purification procedures (Signor *et al.*, 1999). Column fractions were analyzed by SDS-PAGE, and peak fractions were dialyzed into injection buffer and concentrated for microinjection.

Immunocytochemistry

The protocols used for immunofluorescence and immunoblots are described in detail elsewhere (Sharp *et al.*, 1999a). UV vanadate photocleavage was performed as described previously (Hays *et al.*, 1994).

Embryo Microinjections

Microinjections of 0- to 2-h *Drosophila* embryos were carried out as described previously (Sharp *et al.*, 1999b). Briefly, embryos were initially injected with rhodamine-conjugated bovine tubulin (purchased from Molecular Probes, Eugene, OR; or made in our own laboratory), allowed to recover for 5 min, and then injected with antibodies or with control solutions (see below). In our hands, tubulin injections before the cortical migration of nuclei at cycle 10 (the filtrate from spin concentration) often halts development; thus embryos were injected with antibodies during cycle 11. This along with the time delay that occurs between anti-dynein heavy chain (DHC) injections and the earliest resulting defects in spindle pole separation (which were not normally observed until at least prometaphase of cycle 12; see next paragraph) made it impossible for us to assess the effects of anti-DHC injections on interphase–prophase spindle pole movements before cycle 13. For consistency, we limited our analyses of interphase–prophase spindle pole movements in all other conditions to those that occur during cycle 13, as well.

In anti-KLP61F- and anti-DHC-injected embryos, at least one complete cell cycle usually occurred before the first abnormalities were evident; thus our analyses were performed during cycles 12 and 13. Effects of p50 dynamitin injections were generally apparent within one cell cycle after the injection, but embryos were chosen such that spindle pole movements during the same mitotic cycles could be examined. Anti-DHC was injected at concentrations ranging from 8 to 22 mg/ml. Optimal effects were observed at concentrations of $\geq$18 mg/ml; antibody concentrations $\leq$12 mg/ml produced no noticeable effects. p50 dynamitin was injected at 18 mg/ml. For controls, embryos were injected with nonspecific immunoglobulin G or BSA in the same buffer and at the same concentration as the antibodies or p50 dynamitin, respectively. No controls showed the effects described below. In all, 12 wild-type embryos were injected with anti-DHC at optimal concentrations and analyzed in real time. One of these embryos showed no noticeable effects and proceeded through cellularization normally. Two displayed massive nuclear fallout immediately after injection and thus were not analyzed further. The remaining nine embryos all

exhibited defects in spindle pole separation during interphase–prophase of cycle 13 (shown graphically in the Figure 3, top panel). In addition, seven of these exhibited earlier defects during prometaphase–metaphase and anaphase B of cycle 12 (see Figures 4, top right panel, and 5, right panel, respectively). Ten embryos injected with p50 at the appropriate cycles were analyzed, as well. All showed defects similar to anti-DHC-injected embryos. Moreover, nearly all of these embryos displayed a prophase arrest with partially separated spindle poles near the injection site in the cycle after the injection. In addition, 10 ca^{nd} (Ncd null; see *Drosophila* Stocks and Embryo Collections above) embryos were injected with anti-DHC (18 mg/ml) and analyzed. Two were indistinguishable from control injected ca^{nd} embryos, and the remaining eight exhibited wild-type spindle pole separation during cycle 13 and aberrant anaphase B in cycle 12 (see Figure 3, bottom panel). The concentrations of anti-KLP61F antibodies used in this study were the same as described previously (Sharp *et al*., 1999b). In all, 10 wild-type and 10 ca^{nd} embryos were injected with these antibodies, and all displayed the same effects. A single freeze–thaw of either the anti-KLP61F antibodies or anti-DHC destroyed their effects; thus these antibodies were purified and concentrated immediately before use and stored for reuse over the next 1–2 wk at 4°C.

Time-Lapse Laser Scanning Confocal Microscopy

All images were acquired on a Leica (Nussloch, Germany) TCS SP confocal microscope run by the Leica TCS software. Time series were generated using the "Time Series" function contained in the control panel. Each image results from two accumulated (averaged) scans of the sample, and new images were acquired every 5 s. Because changes in the MT arrays of early embryos occur so quickly, all of the images shown and analyzed in this study represent one focal plane (no z-series were performed). This allowed for the highest temporal and spatial resolution with the least amount of bleaching and other damage resulting from multiple laser scans.

Quantitative Image Analysis

After their collection, time series were imported into University of Texas Health Science Center (San Antonio, TX) Image Tool version 2.00 for Windows (downloaded from the Internet at http://ddsdx-.uthscsa.edu/dig/itdesc.html). Nuclei in the half of the embryo surrounding the injection site were analyzed. The distance between spindle poles was determined with the "Distance" tool under the "Analysis" menu in the Image Tool software. In all cases the through-space distance between spindle poles was determined (the length of a straight line drawn between the middle of each spindle pole). To determine the actual extent of spindle pole migration during interphase–prometaphase when spindle poles move circumferentially around the nuclear envelope (see Figures 1A and 3), the arc length (distance traveled by the spindle poles along the curved surface of the nuclear envelope) was derived from the following equation: d = 2*r*Asin(X/2r), where r = radius of the nucleus and X = the through-length between spindle poles. The data shown were acquired from averaging five spindles from two different embryos (10 spindles total). On occasion (10–20% of all embryos observed), massive defects in spindle structure were observed immediately after microinjections. The observed defects, which consisted primarily of multipolar spindles or massive nuclear fallout, occurred with equal frequency in both control and experimental embryos. Thus, we concluded that such defects represented nonspecific effects of microinjection. Because of this, only embryos displaying no obvious defects in spindle structure immediately after antibody, p50, or control injections were included in our analyses. Using this selection criterion, very little variability was observed in the rates of spindle pole movements when measurements were compared between control embryos.

RESULTS

Our goal here was to observe and quantitate the relative activity of a subset of MT motors on spindle pole positioning during the assembly and elongation of bipolar mitotic spindles in *Drosophila* embryos. To this end, we have used time-lapse laser scanning confocal microscopy on embryos containing fluorescently labeled tubulin to measure the extent of spindle pole separation as a function of time in the presence and absence of inhibitors of three mitotic motors, namely the bipolar kinesin KLP61F, the C-terminal kinesin Ncd, and cytoplasmic dynein.

Quantitative Analysis of Mitotic Spindle Pole Positioning in the Drosophila Syncytial Blastoderm

Because the cell cycles in *Drosophila* early embryos become progressively longer as they near cellularization (Foe and Alberts, 1983), it is important to compare spindle pole movements that occur within the same cycle. For technical reasons (see MATERIALS AND METHODS, Embryo Microinjections), in this study we focus on the spindle pole movements that occur in one of the final two cycles before cellularization during three distinct stages in the pathway of mitotic spindle formation and function: 1) interphase–prophase of cycle 13 (the last cycle before cellularization) when duplicated spindle poles migrate to nearly opposite sides of the nuclear envelope; 2) prometaphase–metaphase (between NEB and the onset of anaphase A) of cycle 12; and 3) anaphase B (spindle elongation) of cycle 12. In the quantitative studies presented below, each line plot was derived from the analysis of 10 mitotic spindles from two different embryos (see MATERIALS AND METHODS, Quantitative Image Analysis).

Figure 1A shows plots of spindle pole separation as a function of time during these three stages of mitosis. The top panel plots the positions of pairs of spindle poles, which separate around the nuclear envelope during interphase and prophase and come to lie ~7 μm (arc length) or ~120° apart (Figure 1B). The middle panel (Figure 1A) shows a second phase of spindle pole movements that occur during prometaphase as the spindle elongates from ~7 to ~10 μm (Figure 1, C and D, respectively). Finally, Figure 1A, bottom panel, shows a plot of spindle pole movements that occur during anaphase B when the spindle elongates from ~10 to ~14 μm (Figure 1E). Although it is clear that there is a general trend for the spindle poles to separate throughout mitosis, spindle pole separation does not occur at a linear rate. Instead, the rate of pole separation as reflected in the slopes of the curves in Figure 1 changes in a complex manner with stops, starts, and rate changes.

During the first 300 s of spindle pole migration in interphase–prophase of cycle 13 (Figure 1A, top panel) spindle poles appear to separate in a roughly hyperbolic manner. The initial rate of this separation is ~0.11 μm/s, which gradually slows down to a plateau at ~175–180 s when the spindle poles are ~6 μm apart. After this hyperbolic phase there is a slower, roughly linear rate of spindle pole separation (~0.01 μm/s) during the ensuing 150 s that pushes apart the poles until they lie 7–8 μm apart just before NEB. After NEB in cycle 12, the length of the spindle remains constant (at ~7 μm) for ~25 s and then displays a nearly linear rate of elongation (~0.06 μm/s) driving the poles to a

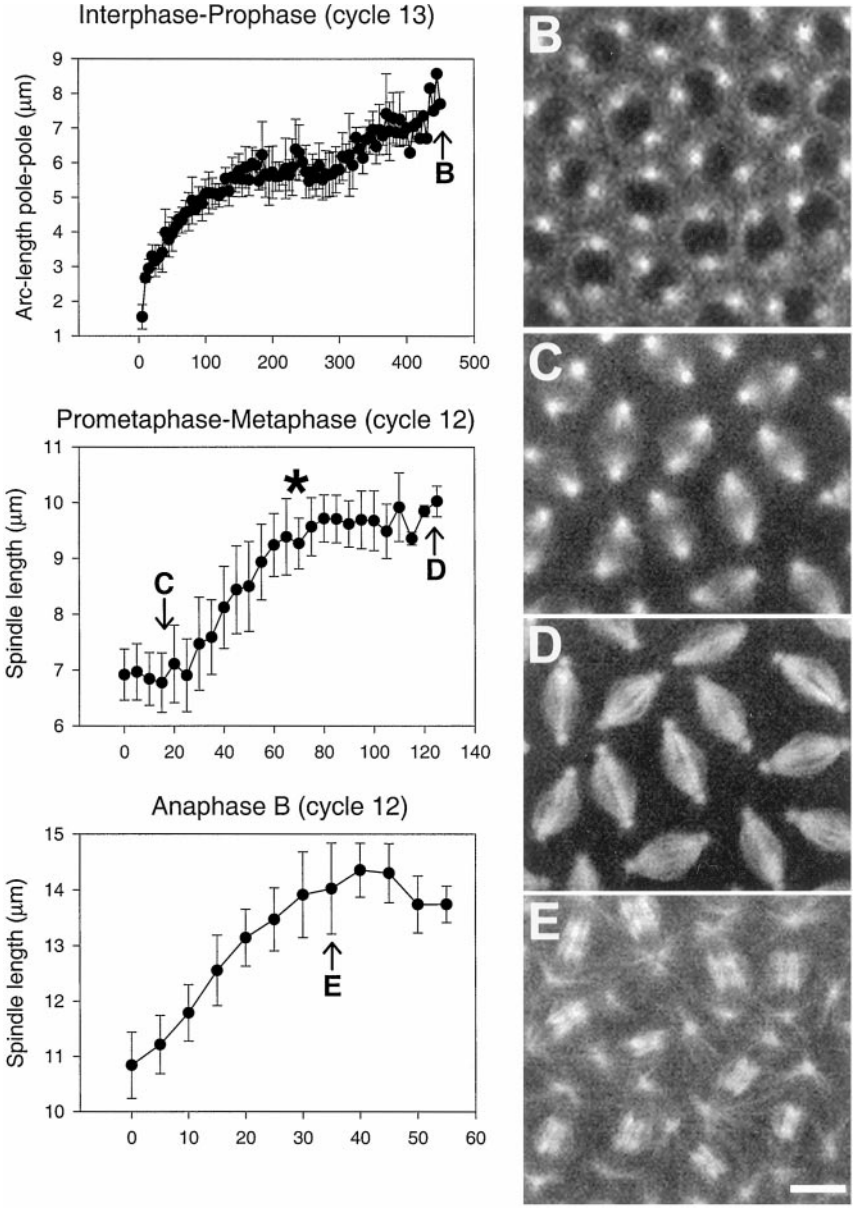

Figure 1. Spindle pole movements in wild-type embryos analyzed in real time. (A) Plots of spindle pole separation versus time during interphase–prophase of cycle 13 (top panel), prometaphase–metaphase of cycle 12 (middle panel), and anaphase B of cycle 12 (bottom panel) in control-injected wild-type *Drosophila* early embryos. Measurements are from time-lapse confocal micrographs taken every 5 s from living *Drosophila* embryos injected with fluorescent tubulin. The star in the middle panel marks the onset of metaphase. (B–E) Still images showing tubulin fluorescence at the time points marked B–E on the plots shown in A. Bar, 7.5 μm. Video for B–E, Mitotic cycles 11–13 in wild-type *Drosophila* embryos: time series of confocal micrographs from a living *Drosophila* embryo injected with fluorescent tubulin. The number of the occurring mitotic cycle is indicated in the top right corner of the video. Actual elapsed time, 25 min 55 s.

separation length of ~10 μm during metaphase (Figure 1A, middle panel). Finally, as anaphase begins there is another nearly linear phase of spindle elongation at a rate of ~0.09 μm/s driving the spindle to reach a peak length of ~14 μm (Figure 1A, bottom panel). Spindle length then decreases slightly during telophase. (A video showing spindle formation during these mitoses can be viewed with Figures 1, B–E.)

A plausible explanation for this complex behavior is that the rate of spindle pole separation remains constant when the net force acting on the poles is constant, whereas any change in the rate reflects a corresponding change in this net force. Specifically, an increase in the rate reflects an enhancement in the net force serving to separate the poles, whereas a decrease in the rate reflects either the decrease in this force or the addition of an antagonistic force that slows spindle pole separation down.

Antagonistic Microtubule Motors Involved in Spindle Pole Migration during Interphase and Prophase

Two motors that might provide force to drive spindle pole separation during the early phases of mitosis are cytoplasmic dynein (Vaisberg *et al.*, 1993; Robinson *et al.*, 1999) and the bipolar kinesin KLP61F (Heck *et al.*, 1993). Our previous studies suggest that KLP61F does not act until the later stages of mitosis (Sharp *et al.*, 1999a,b), and this was supported by our current analyses, which indicate a rate for interphase–prophase spindle pole separation after the injec-

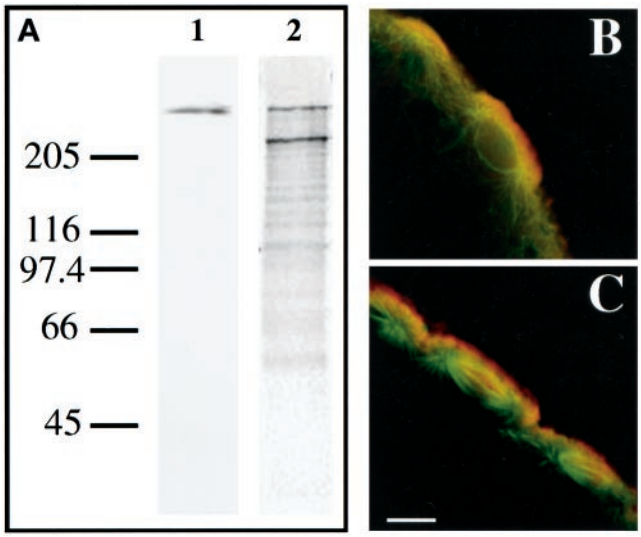

Figure 2. Specificity of the anti-DHC mAb and the immunolocalization of dynein in *Drosophila* early embryos. (A) Immunoblots of purified MAP fractions from *Drosophila* embryonic high-speed supernatant probed with the anti-DHC monoclonal antibody (lane 1) and similar fractions after irradiation with UV light (lane 2) in the presence of Mg-ATP and sodium vanadate. Anti-DHC reacts specifically with one MAP at ~500 kDa, which is sensitive to UV photocleavage in a manner consistent with it being the heavy chain of dynein (Gibbons *et al.*, 1987; Hays *et al.*, 1994; Li *et al.*, 1994). Based on the molecular weight of the cleaved (lower-molecular-weight) band recognized by anti-DHC (lane 2), it is likely that anti-DHC reacts specifically with an epitope contained within the HUV fragment of the dynein heavy chain. Anti-DHC was also used to probe preparations of crude *Drosophila* embryonic cytosol and showed a similarly specific but less intense reactivity (our unpublished results). (B and C) Immunofluorescence of *Drosophila* early embryos double labeled with antibodies against tubulin (green) and the dynein heavy chain (red) during prophase and early anaphase, respectively. Dynein appears to colocalize with the actin-rich cortex or actin caps that surround each nuclear domain. Bar, 3.6 μm.

tion of anti-KLP61F antibodies that is indistinguishable from controls (our unpublished results). Thus, we assessed the role of cytoplasmic dynein in the initial separation of spindle poles. For this, cytoplasmic dynein activity was inhibited in *Drosophila* embryos by two separate methods. In one set of studies we disrupted dynein activity by injecting human p50 dynamitin into *Drosophila* embryos. p50 is a component of the dynein "activator" dynactin (Gill *et al.*, 1991; Schroer and Sheetz, 1991) and has been shown to specifically inhibit cytoplasmic dynein when overexpressed (Echeverri *et al.*, 1996). In a second set of studies, we injected a mAb that specifically recognizes the dynein heavy chain (anti-DHC; Figure 2A) into embryos. Immunofluorescence using anti-DHC shows a cortical staining pattern, very similar to the actin-rich "caps" known to surround each nuclear domain (Warn *et al.*, 1984; Karr and Alberts, 1986; Kellogg *et al.*, 1988), into which the ends of astral MTs extend (Figure 2B). Diffuse staining is also seen on the central spindle but not at the poles after NEB (Figure 2C). For unknown reasons, this localization for the dynein heavy chain in *Drosophila* early embryos is different than that reported previously (Hays *et al.*, 1994), although similar cortical staining has been observed in vertebrate epithelial cells (Busson *et al.*, 1998). Possible explanations for this observation include that anti-DHC is specific for a distinct dynein isoform or recognizes a site on the same dynein isoform that is masked unless the motor is bound to specific cellular targets such as the cortex.

When microinjected into *Drosophila* embryos, both p50 dynamitin and anti-DHC substantially reduce the rate and extent of spindle pole migration during interphase–prophase of cycle 13 (Figure 3, top panel). The initial rapid phase of spindle pole separation is almost completely eliminated, and spindle poles separate to a distance of ~4 and 3 μm in p50- and anti-DHC-injected embryos, respectively, compared with 7 μm in controls. In some cases, the inhibition of dynein also results in a prophase arrest in the affected spindles (see Figure 7, top panel, for video). These data suggest that cytoplasmic dynein located on the cortical actin caps (cortical dynein) exerts pulling forces on astral MTs to provide the major force for spindle pole separation during early phases of mitosis. The inhibition of dynein was also observed to result in the formation of abnormally large nuclei with four associated spindle poles, suggesting defects in karyokinesis (our unpublished results). Such nuclei were never included in our quantitative analyses of spindle pole migration.

Previous studies suggested that the C-terminal kinesin Ncd provides a force that antagonizes the pole-separating activity of the bipolar kinesin KLP61F at stages subsequent to NEB (Sharp *et al.*, 1999b). To determine whether Ncd performs a similar counterbalancing function to cortical dynein in earlier phases of mitosis, we exploited the Ncd null mutant claret-nondisjunctional (ca^{nd}; see MATERIALS AND METHODS, *Drosophila* Stocks and Embryo Collections) (Sturtevant, 1929; Lewis and Gencarella, 1952). Strikingly, the overall rate and extent of spindle pole separation in ca^{nd} embryos is much greater than in wild-type embryos (Figure 3, center panel). Closer analysis reveals that in the absence of Ncd activity the early fast phase of spindle pole separation occurs at roughly the same rate as in wild-type embryos (~0.19 vs. 0.11 μm/s) but overshoots. This overshoot causes the spindle poles to separate nearly completely within the first 100 s of this phase and also results in an overall decrease in the length of each mitotic cycle, in general as illustrated in Figure 4 (see associated video). Based on these observations, we propose that Ncd serves as a brake during the initial migration of spindle poles, limiting its rate and length and preventing the premature separation of spindle poles. This activity may result from the putative capacity of Ncd to cross-link antiparallel microtubules and generate minus-end–directed forces, which would serve to oppose spindle pole separation. In the absence of this control, spindle poles from adjacent nuclei may form aberrant contacts, which could, in turn, result in the formation of microtubule "spurs" often observed between spindles lacking normal Ncd activity (see Figure 4, top right panel, arrow) (Endow and Komma, 1996). The resulting structural instability of these spindles may ultimately decrease the fidelity of chromosome segregation (Endow *et al.*, 1990).

In anti-DHC-microinjected ca^{nd} embryos, we observed a complete rescue to the wild-type rate of spindle pole migration (Figure 3, bottom panel; see Figure 7, bottom

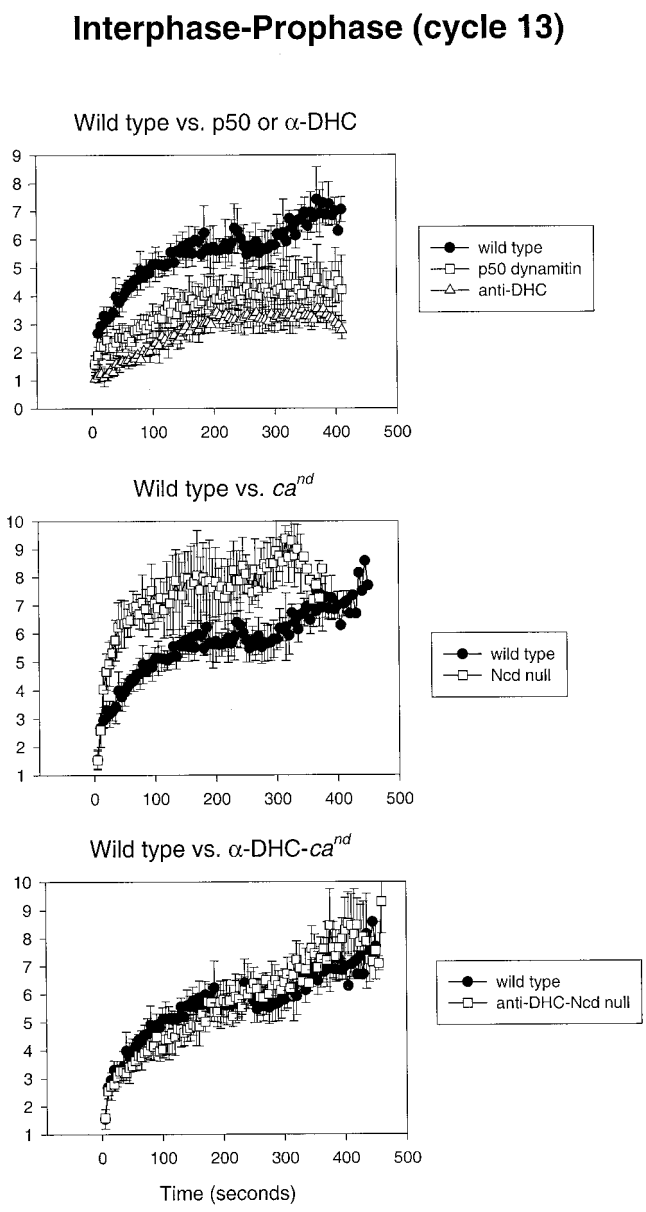

Figure 3. Cytoplasmic dynein and Ncd generate antagonistic forces on spindle poles during interphase–prophase. Top panel, Comparison of spindle pole separation versus time in control-, p50 dynamitin-, and anti-DHC-injected wild-type embryos. Middle panel, Spindle pole separation versus time measured in control-injected wild-type and *ca*nd (Ncd null) embryos. Bottom panel, Spindle pole separation versus time measured in control-injected wild-type and anti-DHC injected *ca*nd embryos.

left panel, for video). The plots of spindle pole migration versus time for the wild-type embryos and anti-DHC-injected *ca*nd embryos after the perturbation of cortical dynein activity are essentially identical. This strongly supports the notion that cytoplasmic dynein and Ncd generate antagonistic forces during the initial separation of spindle poles. Moreover (as discussed below), this observation suggests the existence of an underlying mechanism for spindle pole migration that is independent of cortical dynein and Ncd.

Antagonistic Microtubule Motors Involved in Spindle Pole Separation during Prometaphase and Metaphase

During prometaphase and metaphase of cycle 12, our observations suggest that KLP61F and dynein cooperate to drive the separation of spindle poles, whereas Ncd continues to antagonize this activity by pulling them together. Figure 5, top left panel, shows the temporal sequence of events occurring in wild-type embryos injected with anti-KLP61F antibodies. As previously reported (Sharp *et al.*, 1999b), spindles collapse to form MT monoasters under these conditions. However, our current analyses show that these spindles do not begin to collapse immediately after NEB and maintain a constant spacing of ~7 μm for 25–30 s (similar to controls) before the spindle poles begin to slide together at a rate of ~0.06 μm/s (see Figure 7, top right panel, for video). Figure 5, top right panel, shows the effects of anti-DHC injections during the same stage in spindle formation. Although these spindles do not collapse, the rate and extent of spindle elongation are greatly reduced, with spindles reaching a length at metaphase of only ~8 vs. ~10 μm in controls. Similar results were obtained after the injection of p50 dynamitin (our unpublished results). These observations are consistent with the hypothesis that KLP61F and cortical dynein work in concert to elongate the spindle during prometaphase. Finally, in *ca*nd embryos, the temporal plot of prometaphase–metaphase spindle pole separation appears nearly identical to wild type under control conditions (our unpublished results), but the absence of Ncd activity ameliorates the effects resulting from the injection of anti-KLP61F or anti-DHC antibodies (Figure 5, bottom panels; see Figure 7, bottom right panel, for video). This indicates that Ncd has a role in this process that is antagonistic to both KLP61F and dynein.

Antagonistic Microtubule Motors Involved in Spindle Elongation during Anaphase B

As in prometaphase–metaphase, the activity of both dynein and KLP61F appears to be required for the proper separation of spindle poles during anaphase spindle elongation. Figure 6, top left panel, shows the effects of anti-DHC injection on anaphase B in wild-type embryos. Although spindles are abnormally short in anti-DHC-injected embryos at the onset of anaphase (resulting from an abnormal prometaphase), they elongate at an initial rate that is nearly identical to that observed in controls. However, later anaphase B movements (from 25 to 55 s) are severely hampered, and the spindles shorten significantly, suggesting that dynein is involved in late but not early anaphase B. The mechanical basis for this observation is unclear but may result because, early in anaphase B, spindles are too short to allow extensive contacts to form between astral microtubules and cortical dynein. An entirely similar inhibition of anaphase B was observed in p50-injected embryos, as well (our unpublished results). Figure 6, top right panel, shows the effects of anti-KLP61F

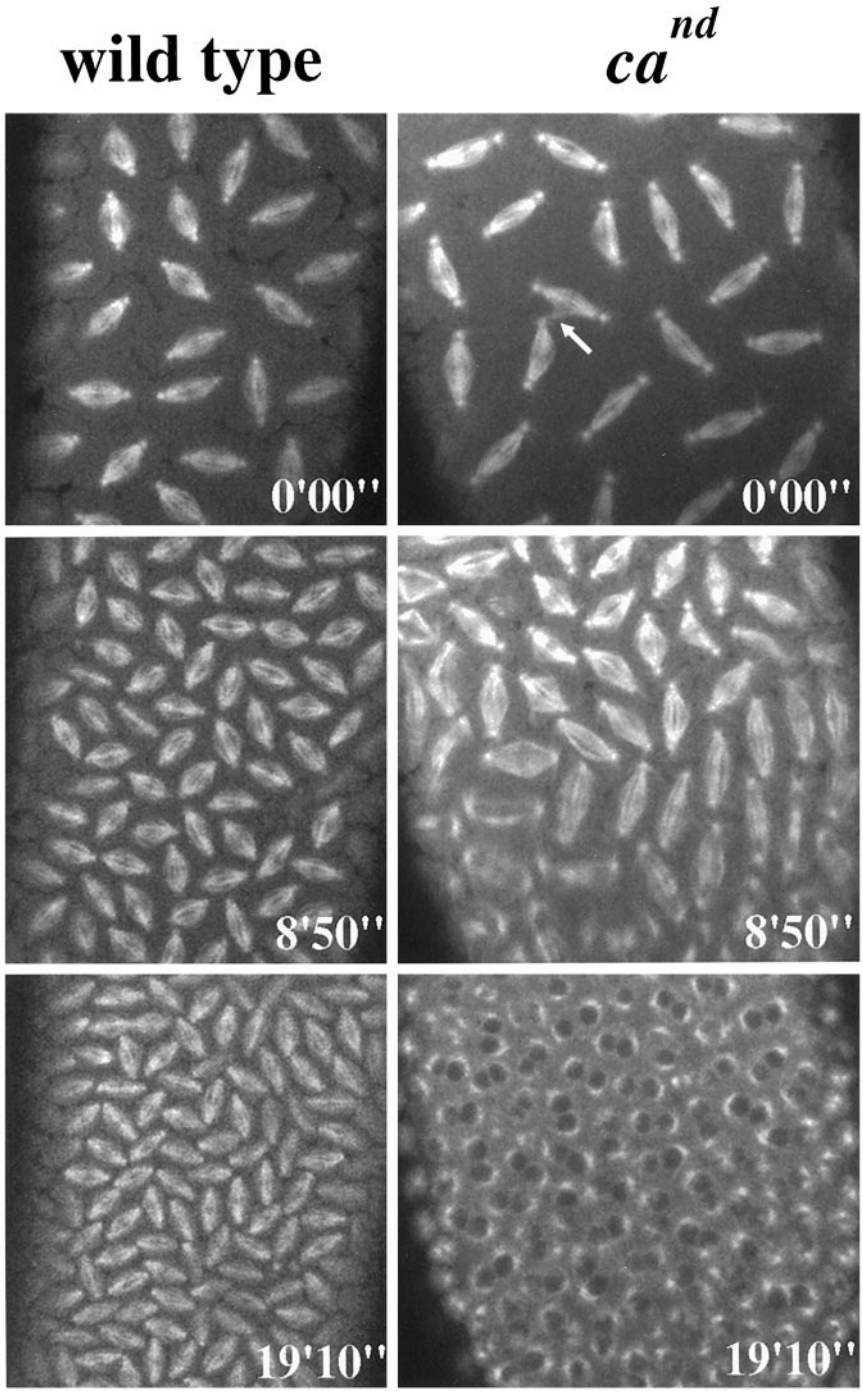

Figure 4. The lack of Ncd activity results in an increased rate of mitosis. Time series images show mitotic spindles from wild-type (left panels) and *ca*nd (right panels) embryos at identical time points. The actual times are indicated at the bottom right of each image. The time series begin with both embryos in metaphase of cycle 11 (the arrow points to a microtubule spur of the type that is often observed to form between *ca*nd spindles; Endow and Komma, 1996). Within 9 min (middle panels) the wild-type embryo has completed one complete mitotic cycle and is in metaphase of cycle 12. By this time point in the *ca*nd embryo, metaphase of cycle 12 is already complete, and anaphase has begun. Note that the interzonal microtubules are clearly disorganized in many *ca*nd spindles. Within 20 min from the onset of the time series (bottom panels) the wild-type embryo has completed a second cycle and is now in metaphase of cycle 13. The *ca*nd embryo, on the other hand, is beginning interphase of cycle 14. Video for left panels, Mitotic cycles 11–13 in *ca*nd *Drosophila* embryos: time series of confocal micrographs from a living *ca*nd injected with fluorescent tubulin. The number of the occurring mitotic cycle is indicated in the top right corner of the video. Actual elapsed time, 24 min 30 s.

injection on anaphase B. Because spindles collapse during prometaphase when KLP61F is inhibited in wild-type embryos, it was necessary to perform this set of experiments in *ca*nd embryos. Overall, under these conditions, both the early and later phases of anaphase B are greatly diminished (although elongation does occur in some spindles), supporting the notion that KLP61F actively drives the apparently dynein-independent early movements in anaphase B. Ncd on its own, however, appears to have little or no influence on anaphase B because, as shown in Figure 6, bottom two panels, the temporal plots of anaphase B in the presence or absence of Ncd activity appear nearly identical in both control and anti-DHC-injected embryos (Figure 6, bottom right and bottom left panels, respectively). Thus, it is possible that anaphase B is triggered by the down-regulation of Ncd, allowing first KLP61F alone and then KLP61F in concert with cortical dynein to drive the poles apart.

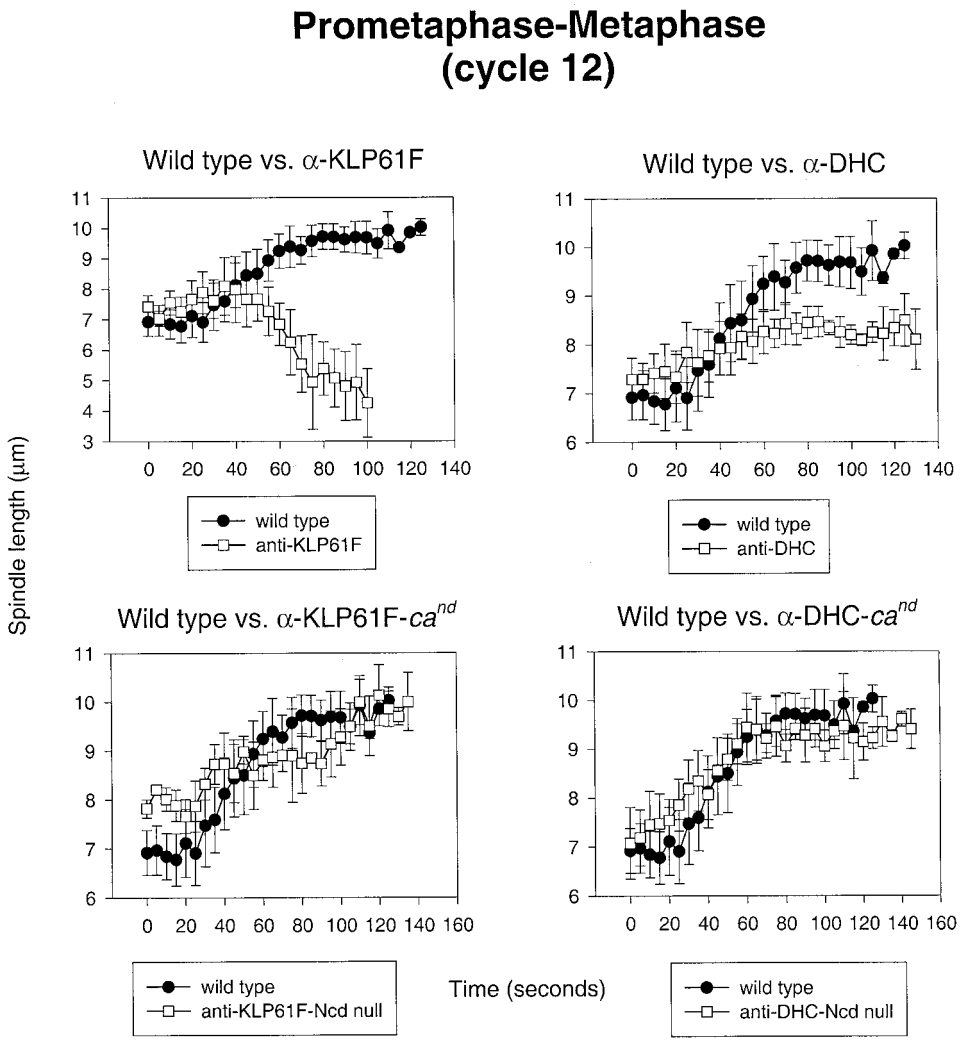

Figure 5. KLP61F and dynein function in concert to separate spindle poles during prometaphase–metaphase and are antagonized by Ncd. Shown is a comparison of spindle pole separation versus time during prometaphase and metaphase in control injected wild-type embryos (all panels), anti-KLP61F-injected wild-type embryos (top left), anti-KLP61F-injected *ca*nd embryos (bottom left), anti-DHC-injected wild-type embryos (top right), and anti-DHC injected *ca*nd embryos (bottom right).

Further experimentation will be required to test the merits of this hypothesis.

Simultaneous Functional Inhibition of Pairs of Antagonistic Motors Uncovers an Underlying "Backup" Mechanism for Mitosis

One striking observation that should be noted is that the inactivation of pairs of counterbalancing MT motors at appropriate stages of mitosis leads to a rescue of successful mitotic spindle assembly and function (Figure 7). For example, the coinhibition of Ncd with dynein (left panels) or Ncd with KLP61F (right panels) results in a nearly complete restoration of normal spindle pole positioning and bipolar spindle assembly during interphase–prophase or prometaphase–metaphase, respectively. Thus, these "double knockouts" may have uncovered underlying mechanisms for bipolar spindle assembly and maintenance before anaphase. Although the identity of these backup mechanisms is unknown, possibilities include: 1) a low level of residual KLP61F or dynein motor activity that is sufficient to drive spindle formation in the absence of the antagonistic forces generated by Ncd; 2) redundant sets of MT motors whose activities are normally masked by dynein, KLP61F, and Ncd; 3) the force derived from MT dynamics; 4) interactions between MTs and the dynamic actin network that surrounds the spindle; and 5) a novel, unidentified mechanical system that contributes to mitosis.

DISCUSSION

In this study, we performed a series of real-time quantitative analyses to assess how the activities of three mitotic motors are coordinated to appropriately position spindle poles during mitosis. To accomplish this it was necessary to quantitate spindle assembly with a higher temporal resolution than has previously been accomplished in animal cells. This approach revealed that, in control embryos, there is a general trend for the spindle poles to separate throughout mitosis, but the rate of pole separation is nonlinear, suggesting that the net forces acting on the poles are not constant. Quantitation of spindle

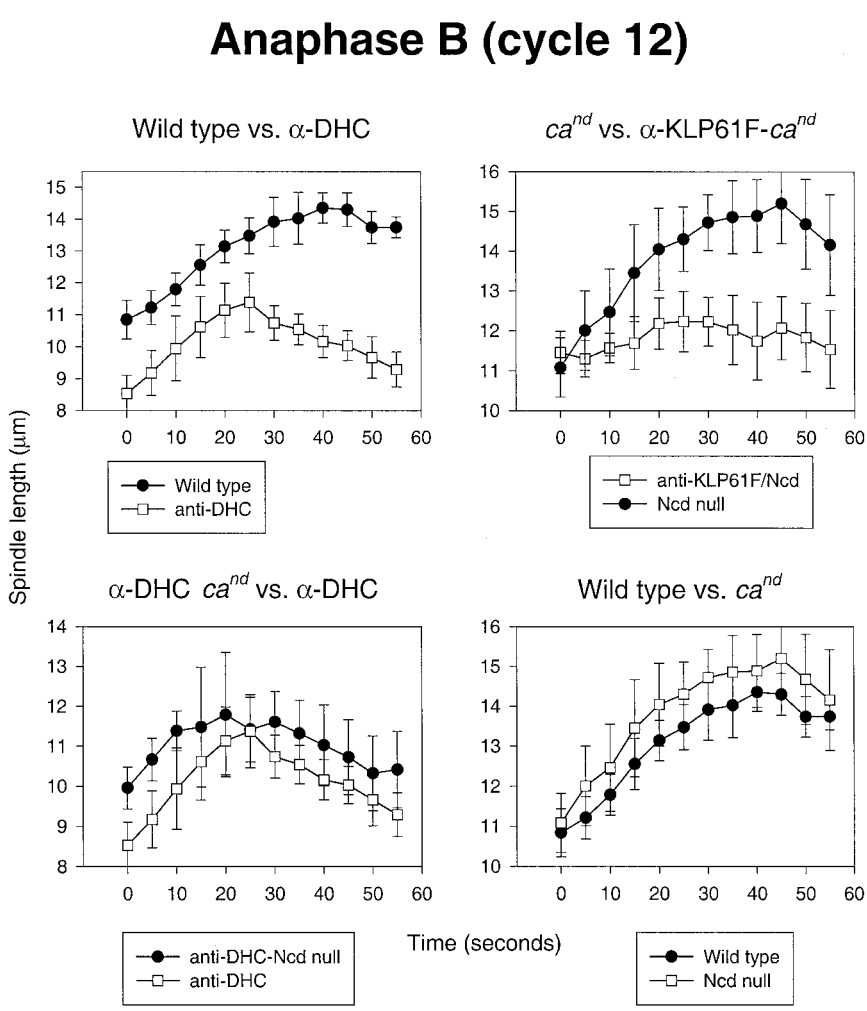

Figure 6. Dynein and KLP61F drive anaphase B spindle elongation. Comparison of spindle pole separation versus time during anaphase B is shown. Top left panel, Control-injected wild-type embryos versus anti-DHC-injected wild-type embryos. Bottom left panel, anti-DHC-injected wild-type embryos versus anti-DHC-injected *ca*nd embryos. Top right panel, Control-injected *ca*nd embryos versus anti-KLP61F-injected *ca*nd embryos. Bottom right panel, Control-injected wild-type embryos versus control-injected *ca*nd embryos.

pole movements in the presence of various combinations of specific inhibitors of cytoplasmic dynein, Ncd, and KLP61F has indicated that spindle pole positioning is precisely controlled by a carefully orchestrated balance of forces that results from the combined activities of these three motors. The potential mechanistic details of this balance will be discussed in greater detail below (see Figure 8).

Model: Coordinated Sliding Filament Mechanisms in the Pathway of Mitosis

Nearly 30 years ago it was proposed that mitosis was driven by a sliding filament mechanism in which force-generating enzymes cross-link adjacent spindle MTs and slide them in relation to one another (McIntosh *et al.*, 1969; McDonald *et al.*, 1977). The results reported in this and previous studies suggest that the three MT motor proteins analyzed here, dynein, the C-terminal kinesin Ncd, and the bipolar kinesin KLP61F, cooperate in such a mechanism to drive bipolar spindle assembly and elongation (Figure 8). Previous studies have shown that both KLP61F and Ncd localize to interpolar MT bundles where they can cross-link antiparallel MTs and slide them in relation to one another (Endow and Komma, 1996; Sharp *et al.*, 1999a). The immunolocalization of dynein to the cortical actin caps, shown here, is consistent with the hypothesis that this motor functions by a modification of the sliding filament mechanism, cross-linking, and sliding astral MTs in relation to the fixed actin cortex. It has also been proposed that the association between dynein and the cortex occurs via dynactin (Karki and Holzbaur, 1999), which may explain the similar effects resulting from anti-DHC and p50 dynamitin injections. Given that spindle MTs are oriented with their minus ends focused at the poles (Euteneuer *et al.*, 1982), these activities would allow the plus-end–directed KLP61F and the minus-end–directed cortical dynein to push and pull the poles apart, respectively, while allowing the minus-end–directed Ncd to act as a brake or counterbalance and pull the poles together.

Our data suggest the following functional relationships among dynein, KLP61F, and Ncd during the pathway of spindle assembly and elongation (shown schematically in Figure 8). During the initial migration of spindle poles in interphase–prophase, the activity of dynein, which is anchored to the cortex by dynactin, provides the major pole separation force as KLP61F is sequestered in the nucleus

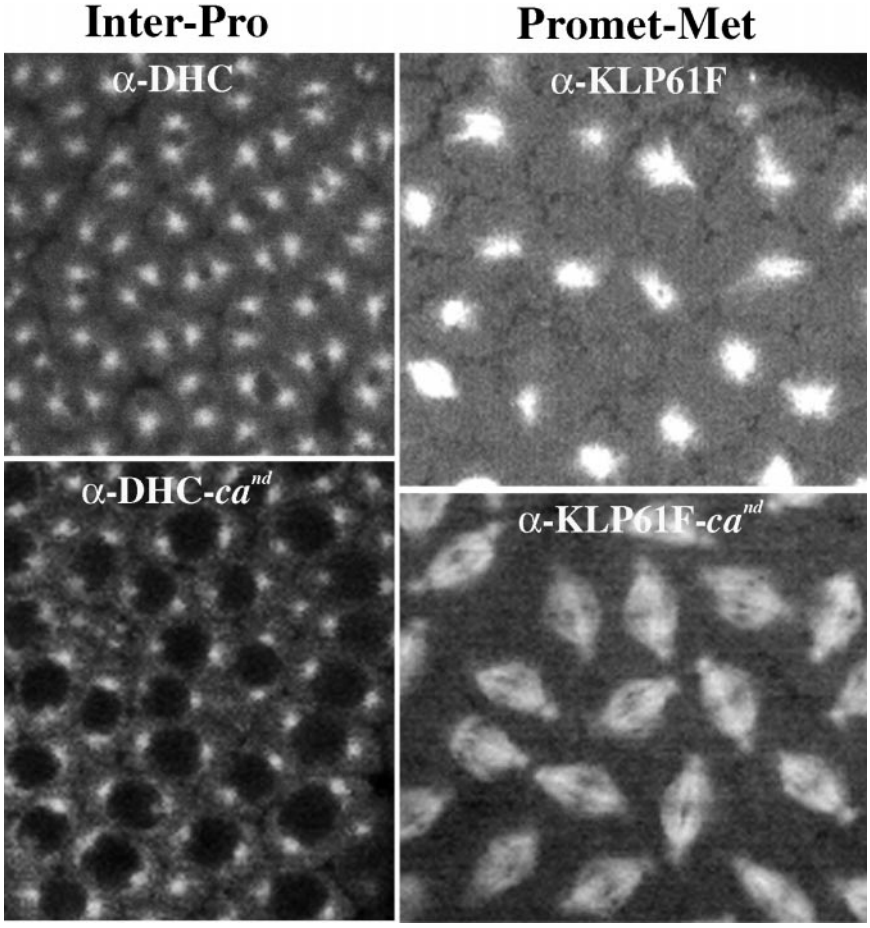

Figure 7. Spindle defects induced by inhibiting either dynein or KLP61F are reversed by double knockouts with Ncd. Confocal micrographs from live wild-type embryos coinjected with fluorescent tubulin and anti-DHC (top left) or anti-KLP61F (top right) are shown. The inhibition of dynein results in only partial spindle pole separation during interphase–prophase, and the inhibition of KLP61F results in spindle collapse during prometaphase. Bottom panels show the same time points in ca^{nd} embryos treated similarly. In the absence of both dynein and Ncd or KLP61F and Ncd the spindles form and function relatively normally through metaphase. Bar, 6 μm. Video for top left panel, Inhibition of spindle pole separation after the inhibition of cytoplasmic dynein: interphase–prophase of cycle 13 in a wild-type embryo injected with anti-DHC. Near the injection site (at the extreme left of the field shown in the video), nuclei arrest in prophase with partially separated spindle poles. At sites distal to the injection site, some nuclei attempt to undergo mitosis. In this video, some nuclei are positioned extremely close to one another because of aberrant anaphase B during the previous cycle (cycle 12). Actual elapsed time, 13 min 20 s. Video for top right panel, Collapse of bipolar spindles during prometaphase after the inhibition of KLP61F: Interphase–prophase and prometaphase of cycle 12 in a wild-type embryo injected with anti-KLP61F antibodies. Actual elapsed time, 4 min 20 s. Video for bottom left panel, Rescue of spindle pole separation by coinhibition of cytoplasmic dynein with Ncd: interphase–prophase of cycle 13 in ca^{nd} embryo injected with anti-DHC. Actual elapsed time, 8 min 20 s. Video for bottom right panel, Rescue of spindle collapse by coinhibition of KLP61F with Ncd: cycle 12 in ca^{nd} embryo injected with anti-KLP61F antibodies. Actual elapsed time, 4 min 20 s.

(Sharp *et al.*, 1999a) and thus cannot participate in these movements. Ncd antagonizes dynein-driven spindle pole migration, gradually slowing the rate of spindle pole movements by using its ability to cross-link MTs between the poles to serve as a brake. After NEB, the activity of dynein is augmented by KLP61F, which is now capable of cross-linking antiparallel MTs within interpolar MT bundles and exerting pushing forces that contribute to pole separation. We propose that during this time the main function of KLP61F is to counterbalance Ncd, maintaining the spindle under isometric tension and preventing spindle collapse. The augmentation of the activity of KLP61F with that of dynein, however, overrides the balance between KLP61F and Ncd and drives a rapid, linear rate of spindle pole separation that ends when a new isometric balance between the three motors is reached at metaphase (alternatively, the pause in spindle pole movements during metaphase may be the result of stable bipolar attachments between spindle microtubules and chromosomes that are established at approximately the same point in the cell cycle). Finally, during anaphase, our data suggest that the activity of Ncd may be decreased or turned off. If this is indeed the case, this decrease may tip the isometric balance established at metaphase, allowing the additive effects of pushing forces driven by KLP61F on interpolar MT bundles together with pulling forces driven by cortical dynein on astral MT to drive anaphase B spindle elongation.

Experimental Rationale

To carry out the studies that led to our model, it was necessary for us to inhibit dynein and KLP61F by way of antibody microinjections. Dynein was also inhibited by the microinjection of p50 dynamitin. This approach allowed us to control when the inhibition of these motors occurs, assuming, of course, that the injected antibodies quickly bind and inactivate their intended targets. Although we are aware of the caveats, as well as the strengths, of antibody microinjection experiments (Scholey, 1998), we consider it likely that the antibodies used in this study strongly and specifically inhibit the activities of dynein and KLP61F for the following reasons. First, the microinjection of our anti-DHC or anti-KLP61F antibodies produced effects on spindle pole positioning that are similar to those reported in KLP61F (Heck *et al.*, 1993) and dynein (Robinson *et al.*, 1999) mutants. Second, in the case of dynein, two different inhibitors, anti-DHC and p50 dynamitin, produced strikingly similar results.

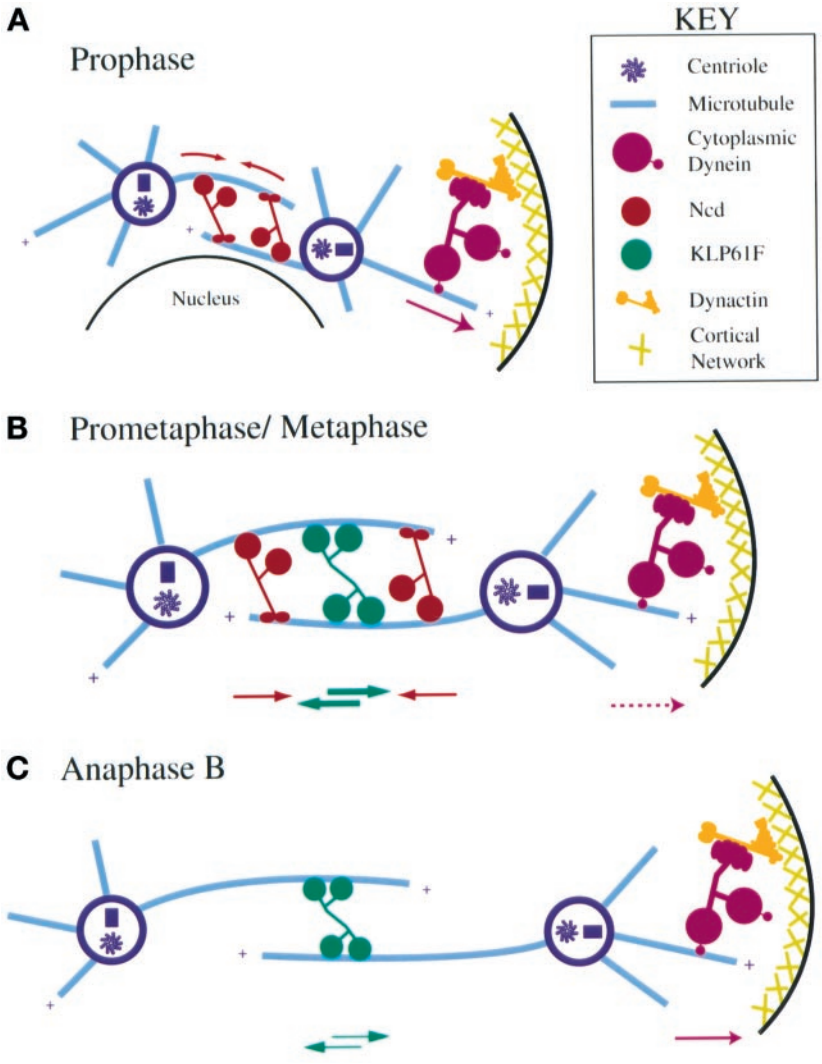

Figure 8. Model: pathway of spindle pole positioning determined by dynein, KLP61F, and Ncd activity during mitosis. Schematic illustrations depict the proposed timing and mechanism of action for dynein, KLP61F, and Ncd during the assembly and function of mitotic spindles in *Drosophila* early embryos. (A) Prophase. Dynein, anchored to the cortex by dynactin, pulls on astral MTs to separate spindle poles, whereas Ncd cross-links and slides together antiparallel MTs between the spindle poles to act as a brake. KLP61F is sequestered in the nucleus and does not participate in these movements. (B) Prometaphase/Metaphase. After NEB, KLP61F can cross-link and slide apart antiparallel MTs balancing the "inward" force generated by Ncd on these same MTs and offsetting spindle collapse. Cortical dynein pulls on astral MTs and in concert with KLP61F drives prometaphase spindle elongation. (C) Anaphase B. The inactivation of Ncd at anaphase allows KLP61F and cortical dynein to drive the poles farther apart. KLP61F appears to act before dynein in this process.

In theory, these studies could also be performed using the mutational inhibition of dynein and KLP61F. However, because severe loss-of-function mutations in the genes encoding these motors are lethal, and because maternal transcripts and proteins are loaded into early embryos (O'Farrell *et al.*, 1989), we thought that this approach would not be appropriate for our purposes. Therefore, only Ncd, which is not essential for the survival of embryos or the formation of spindles, was inhibited genetically. We note that an added benefit of using antibody microinjections in mutant backgrounds (e.g., anti-dynein in Ncd null mutants) is that they can be used to generate double knockouts.

Relationship of Our Results to Previous Studies

The functions of dynein, KLP61F, and Ncd have been assessed in *Drosophila* early embryos in two recent studies. In the first of these, it was shown that KLP61F and Ncd generate antagonistic forces to position mitotic spindle poles after NEB (Sharp *et al.*, 1999b). More recently, it was shown that hypomorphic mutations in the dynein heavy chain reduced the extent of spindle pole separation during interphase–prophase in this system (Robinson *et al.*, 1999). Although the roles of dynein, KLP61F, and Ncd are also reported here, the important novel feature of our work is to show how the activities of these motors are organized into an ordered pathway for spindle assembly and function.

The functions of cytoplasmic dynein, bipolar kinesins, and C-terminal kinesins have also been studied extensively in fungi, but the results of those studies leave many unanswered questions, some of which are addressed here. First, we show that cytoplasmic dynein is involved in positioning spindle poles throughout all stages of spindle assembly and elongation; because dynein is not necessary for proper spindle pole separation before anaphase in fungi (Eshel *et al.*, 1993; Li *et al.*, 1993; Xiang *et al.*, 1994; Yeh *et al.*, 1995), its role(s) in the early stages of mitosis could not be examined. Second, we show that the *Drosophila* C-terminal kinesin Ncd constrains the rate of spindle pole separation during spindle

assembly; similar kinetic analyses have not been performed in fungi, probably because of the small size of preanaphase fungal spindles. Third, we show that Ncd acts antagonistically to both dynein and the bipolar kinesin KLP61F; although the latter interaction has been carefully characterized in fungal systems (Saunders and Hoyt, 1992; Saunders *et al.*, 1997; Hoyt *et al.*, 1993; O'Connell *et al.*, 1993; Pidoux *et al.*, 1996), the former has not been reported previously. Finally, we show with high temporal resolution how dynein and KLP61F cooperate to elongate the spindle during prometaphase and anaphase. Specifically, our data suggest that KLP61F is inactive before NEB (Sharp *et al.*, 1999a,b), but then it exerts a stronger influence on spindle pole positioning during prometaphase and acts earlier during anaphase B than dynein. Although studies in fungi have also revealed that bipolar kinesins and dynein cooperate during spindle elongation (Saunders *et al.*, 1995), their specific temporal relationships in this process were not determined.

Concluding Remarks

Our studies reveal functional relationships between three mitotic motors (Figure 8) and show that nearly every major change in the elongation rate of *Drosophila* embryonic mitotic spindles can be associated with the addition or subtraction of dynein, KLP61F, or Ncd activity. However, our observation that the inhibition of pairs of antagonistic motors rescues spindle activity (at least through metaphase) suggests that these three motors are not the only factors involved in this process and may unmask a redundant mechanism for bipolar spindle assembly and maintenance (although the activity of a residual pool of active motors after antibody microinjections cannot be ruled out as the driving force behind this). Future studies should be aimed at elucidating the molecular mechanisms and function of this redundant process, as well as probing, in more detail, the precise structural mechanisms by which dynein, C-terminal kinesins, and bipolar kinesins cooperate to drive bipolar spindle assembly and elongation. Such endeavors may be assisted significantly by the use of high-resolution "real-time" quantitative analyses of living organisms, such as those reported here.

ACKNOWLEDGMENTS

We thank Drs. Frank McNally, Lesilee Rose, Bo Liu, and Peter Baas for critically reading the manuscript, Melanie Tomczak for help with the data analysis, and Dr. Heiner Matthies for technical advice regarding the purification of p50 dynamitin. This work was supported by grant GM-55507 from the National Institutes of Health to J.M.S. and postdoctoral fellowship GM-19262 from the National Institutes of Health to D.J.S. The anti-DHC antibody was made and characterized by Daniel Rines.

REFERENCES

Blangy, A., Lane, H.A., d'Herin, P., Harper, M., Kress, M., and Nigg, E.A. (1995). Phosphorylation by p34cdc2 regulates spindle association of human Eg5, a kinesin-related motor essential for bipolar spindle formation in vivo. Cell *83*, 1159–1169.

Bloom, K.S., Beach, D.L., Maddox, P., Shaw, S.L., Yeh, E., and Salmon, E.D. (1999). Using green fluorescent protein fusion proteins to quantitate microtubule and spindle dynamics in budding yeast. Methods Cell Biol. *61*, 369–383.

Busson, S., Dujardin, D., Moreau, A., Dompierre, J., and De Mey, J.R. (1998). Dynein and dynactin are localized to astral microtubules and at cortical sites in mitotic epithelial cells. Curr. Biol. *8*, 541–544.

Chandra, R., Salmon, E.D., Erickson, H.P., Lockhart, A., and Endow, S.A. (1993). Structural and functional domains of the *Drosophila* Ncd microtubule motor protein. J. Biol. Chem. *268*, 9005–9013.

Cole, D.G., Saxton, W.M., Sheehan, K.B., and Scholey, J.M. (1994). A "slow" homotetrameric kinesin-related motor protein purified from *Drosophila* embryos. J. Biol. Chem. *269*, 22913–22916.

Echeverri, C.J., Paschal, B.M., Vaughan, K.T., and Vallee, R.B. (1996). Molecular characterization of the 50-kDa subunit of dynactin reveals function for the complex in chromosome alignment and spindle organization during mitosis. J. Cell Biol. *132*, 617–633.

Endow, S.A., Henikoff, S., and Soler-Niedziela, L. (1990). Mediation of meiotic and early mitotic chromosome segregation in *Drosophila* by a protein related to kinesin. Nature *345*, 81–83.

Endow, S.A., Kang, S.J., Satterwhite, L.L., Rose, M.D., Skeen, V.P., and Salmon, E.D. (1994). Yeast Kar3 is a minus-end microtubule motor protein that destabilizes microtubules preferentially at the minus ends. EMBO J. *13*, 2708–2713.

Endow, S.A., and Komma, D.J. (1996). Centrosome and spindle function of the *Drosophila* Ncd microtubule motor visualized in live embryos using Ncd-GFP fusion proteins. J. Cell Sci. *109*, 2429–2442.

Enos, A.P., and Morris, N.R. (1990). Mutation of a gene that encodes a kinesin-like protein blocks nuclear division in *A. nidulans*. Cell *60*, 1019–1027.

Eshel, D., Urrestarazu, L.A., Vissers, S., Jauniaux, J.C., van Vliet-Reedijk, J.C., Planta, R.J., and Gibbons, I.R. (1993). Cytoplasmic dynein is required for normal nuclear segregation in yeast. Proc. Natl. Acad. Sci. USA *90*, 11172–11176.

Euteneuer, U., Jackson, W.T., and McIntosh, J.R. (1982). Polarity of spindle microtubules in *Hemanthus* endosperm. J. Cell Biol. *94*, 644–653.

Foe, V.E., and Alberts, B.M. (1983). Studies of nuclear and cytoplasmic behavior during the five mitotic cycles that precede gastrulation in *Drosophila* embryogenesis. J. Cell Sci. *61*, 31–70.

Gibbons, I.R., Lee-Eiford, A., Mocz, G., Phillipson, C.A., Tang, W.J., and Gibbons, B.H. (1987). Photosensitized cleavage of dynein heavy chains. Cleavage at the "V1 site" by irradiation at 365 nm in the presence of ATP and vanadate. J. Biol Chem. *262*, 2780–2786.

Gill, S.R., Schroer, T.A., Szilak, I., Steuer, E.R., Sheetz, M.P., and Cleveland, D.W. (1991). Dynactin, a conserved, ubiquitously expressed component of an activator of vesicle motility mediated by cytoplasmic dynein. J. Cell Biol. *115*, 1639–1650.

Gordon, D.M., and Roof, D.M. (1999). The kinesin-related protein Kip1p of *Saccharomyces cerevisiae* is bipolar. J. Biol. Chem. *274*, 28779–28786.

Hagan, I., and Yanagida, M. (1990). Novel potential mitotic motor protein encoded by the fission yeast cut7+ gene. Nature *347*, 563–566.

Harlow, E., and Lane, D. (1988). Monoclonal antibodies. In: Antibodies: A Laboratory Manual, Cold Spring Harbor, NY: Cold Spring Harbor Laboratory Press, 141–243.

Hays, T.S., Porter, M.E., McGrail, M., Grissom, P., Gosch, P., Fuller, M.T., and McIntosh, J.R. (1994). A cytoplasmic dynein motor in *Drosophila*: identification and localization during embryogenesis. J. Cell Sci. *107*, 1557–1569.

Heald, R., Tournebize, R., Blank, T., Sandaltzopoulos, R., Becker, P., Hyman, A., and Karsenti, E. (1996). Self-organization of microtubules into bipolar spindles around artificial chromosomes in *Xenopus* egg extracts [see comments]. Nature *382*, 420–425.

Heck, M.M., Pereira, A., Pesavento, P., Yannoni, Y., Spradling, A.C., and Goldstein, L.S. (1993). The kinesin-like protein KLP61F is essential for mitosis in *Drosophila*. J. Cell Biol. *123*, 665–679.

Hoyt, M.A., and Geiser, J.R. (1996). Genetic analysis of the mitotic spindle. Annu. Rev. Genet. *30*, 7–33.

Hoyt, M.A., He, L., Loo, K.K., and Saunders, W.S. (1992). Two *Saccharomyces cerevisiae* kinesin-related gene products required for mitotic spindle assembly. J. Cell Biol. *118*, 109–120.

Hoyt, M.A., He, L., Totis, L., and Saunders, W.S. (1993). Loss of function of *Saccharomyces cerevisiae* kinesin-related CIN8 and KIP1 is suppressed by KAR3 motor domain mutations. Genetics *135*, 35–44.

Karabay, A., and Walker, R.A. (1999). Identification of microtubule binding sites in the Ncd tail domain. Biochemistry *38*, 1838–1849.

Karki, S., and Holzbaur, E.L. (1999). Cytoplasmic dynein and dynactin in cell division and intracellular transport. Curr. Opin. Cell Biol. *11*, 45–53.

Karr, T.L., and Alberts, B.M. (1986). Organization of the cytoskeleton in early *Drosophila* embryos. J. Cell Biol. *102*, 1494–1509.

Karsenti, E., Boleti, H., and Vernos, I. (1996). The role of microtubule dependent motors in centrosome movements and spindle pole organization during mitosis. Semin. Cell Dev. Biol. *7*, 367–378.

Kashina, A.S., Baskin, R.J., Cole, D.G., Wedaman, K.P., Saxton, W.M., and Scholey, J.M. (1996a). A bipolar kinesin. Nature *379*, 270–272.

Kashina, A.S., Scholey, J.M., Leszyk, J.D., and Saxton, W.M. (1996b). An essential bipolar mitotic motor [letter]. Nature *384*, 225.

Kellogg, D.R., Mitchison, T.J., and Alberts, B.M. (1988). Behavior of microtubules and actin filaments in living *Drosophila* embryos. Development *103*, 675–686.

Lewis, E.B., and Gencarella, W. (1952). Claret and nondisjunction in *Drosophila melanogaster*. Genetics *37*, 600–601.

Li, M., McGrail, M., Serr, M., and Hays, T.S. (1994). *Drosophila* cytoplasmic dynein, a microtubule motor that is asymmetrically localized in the oocyte. J. Cell Biol. *126*, 1475–1494.

Li, Y.Y., Yeh, E., Hays, T., and Bloom, K. (1993). Disruption of mitotic spindle orientation in a yeast dynein mutant. Proc. Natl. Acad. Sci. USA *90*, 10096–10100.

McDonald, H.B., and Goldstein, L.S. (1990). Identification and characterization of a gene encoding a kinesin-like protein in *Drosophila*. Cell *61*, 991–1000.

McDonald, H.B., Stewart, R.J., and Goldstein, L.S. (1990). The kinesin-like ncd protein of *Drosophila* is a minus end-directed microtubule motor. Cell *63*, 1159–1165.

McDonald, K., Pickett-Heaps, J.D., McIntosh, J.R., and Tippit, D.H. (1977). On the mechanism of anaphase spindle elongation in *Diatoma vulgare*. J. Cell Biol. *74*, 377–388.

McIntosh, J.R., Hepler, P.K., and Van Wie, D.G. (1969). Model for mitosis. Nature *224*, 659–663.

McIntosh, J.R., and McDonald, K.L. (1989). The mitotic spindle. Sci. Am. *261*, 48–56.

Meluh, P.B., and Rose, M.D. (1990). KAR3, a kinesin-related gene required for yeast nuclear fusion. Cell *60*, 1029–1041 (erratum *61*, 548).

Narasimhulu, S.B., and Reddy, A.S. (1998). Characterization of microtubule binding domains in the *Arabidopsis* kinesin-like calmodulin binding protein. Plant Cell *10*, 957–965.

O'Connell, M.J., Meluh, P.B., Rose, M.D., and Morris, N.R. (1993). Suppression of the bimC4 mitotic spindle defect by deletion of klpA, a gene encoding a KAR3-related kinesin-like protein in *Aspergillus nidulans*. J. Cell Biol. *120*, 153–162.

O'Farrell, P.H., Edgar, B.A., Lakich, D., and Lehner, C.F. (1989). Directing cell division during development. Science *246*, 635–640.

Pidoux, A.L., LeDizet, M., and Cande, W.Z. (1996). Fission yeast pkl1 is a kinesin-related protein involved in mitotic spindle function. Mol. Biol. Cell *7*, 1639–1655.

Robinson, J.T., Wojcik, E.J., Sanders, M.A., McGrail, M., and Hays, T.S. (1999). Cytoplasmic dynein is required for the nuclear attachment and migration of centrosomes during mitosis in *Drosophila*. J. Cell Biol. *146*, 597–608.

Roof, D.M., Meluh, P.B., and Rose, M.D. (1991). Multiple kinesin-related proteins in yeast mitosis. Cold Spring Harb. Symp. Quant. Biol. *56*, 693–703.

Saunders, W., Lengyel, V., and Hoyt, M.A. (1997). Mitotic spindle function in *Saccharomyces cerevisiae* requires a balance between different types of kinesin-related motors. Mol. Biol Cell. *8*, 1025–1033.

Saunders, W.S., and Hoyt, M.A. (1992). Kinesin-related proteins required for structural integrity of the mitotic spindle. Cell *70*, 451–458.

Saunders, W.S., Koshland, D., Eshel, D., Gibbons, I.R., and Hoyt, M.A. (1995). *Saccharomyces cerevisiae* kinesin- and dynein-related proteins required for anaphase chromosome segregation. J. Cell Biol. *128*, 617–624.

Sawin, K.E., LeGuellec, K., Philippe, M., and Mitchison, T.J. (1992). Mitotic spindle organization by a plus-end-directed microtubule motor. Nature *359*, 540–543.

Scholey, J.M. (1998). Functions of motor proteins in echinoderm embryos: an argument in support of antibody inhibition experiments. Cell Motil. Cytoskeleton *39*, 257–260.

Schroer, T.A., and Sheetz, M.P. (1991). Two activators of microtubule-based vesicle transport. J. Cell Biol. *115*, 1309–1318.

Sharp, D.J., McDonald, K.L., Brown, H.M., Matthies, H.J., Walczak, C., Vale, R.D., Mitchison, T.J., and Scholey, J.M. (1999a). The bipolar kinesin, KLP61F, cross-links microtubules within interpolar microtubule bundles of *Drosophila* embryonic mitotic spindles. J. Cell Biol. *144*, 125–138.

Sharp, D.J., Yu, K.R., Sissons, J.C., Sullivan, W., Scholey, J.M. (1999b). Antagonistic microtubule sliding motors position mitotic centrosomes in *Drosophila* early embryos. Nature Cell Biol. *1*, 51–54.

Signor, D., Wedaman, K.P., Rose, L.S., and Scholey, J.M. (1999). Two heteromeric kinesin complexes in chemosensory neurons and sensory cilia of *Caenorhabditis elegans*. Mol. Biol. Cell *10*, 345–360.

Straight, A.F., Sedat, J.W., and Murray, A.W. (1998). Time-lapse microscopy reveals unique roles for kinesins during anaphase in budding yeast. J. Cell Biol. *143*, 687–694.

Sturtevant, A.H. (1929). The claret mutant type of *Drosophila simulans:* a study of chromosome elimination and of cell-lineage. Z. Wiss. Zool. *135*, 323–356.

Vaisberg, E.A., Koonce, M.P., and McIntosh, J.R. (1993). Cytoplasmic dynein plays a role in mammalian mitotic spindle formation. J. Cell Biol. *123*, 849–858.

Vale, R.D., and Fletterick, R.J. (1997). The design plan of kinesin motors. Annu. Rev. Cell Dev. Biol. *13*, 745–777.

Walker, R.A., Salmon, E.D., and Endow, S.A. (1990). The *Drosophila* claret segregation protein is a minus-end directed motor molecule. Nature *347*, 780–782.

Warn, R.M., Magrath, R., and Webb, S. (1984). Distribution of F-actin during cleavage of the *Drosophila* syncytial blastoderm. J. Cell Biol. *98*, 156–162.

Xiang, X., Beckwith, S.M., and Morris, N.R. (1994). Cytoplasmic dynein is involved in nuclear migration in *Aspergillus nidulans*. Proc. Natl. Acad. Sci. USA *91*, 2100–2104.

Yeh, E., Skibbens, R.V., Cheng, J.W., Salmon, E.D., and Bloom, K. (1995). Spindle dynamics and cell cycle regulation of dynein in the budding yeast, *Saccharomyces cerevisiae*. J. Cell Biol. *131*, 687–700.